EPJ Web of Conferences **192**, 00015 (2018) https://doi.org/10.1051/epjconf/201819200015
QCD@Work 2018

Measurements of open charm production and flow in $\sqrt{s_{\rm NN}}$ = 200 GeV Au+Au collisions with the STAR experiment at RHIC

Spyridon Margetis[1,*] for the STAR Collaboration

[1]Department of Physics, Kent State University, Ohio 44242, USA

Abstract. We present an improved, higher statistics, measurement with respect to the previously published results of the D^0 meson elliptic flow (v_2) as a function of transverse momentum (p_T) in Au+Au collisions at $\sqrt{s_{\rm NN}}$ = 200 GeV with the STAR Heavy Flavor Tracker (HFT). The D^0 v_2 results are compared to those of light-flavor hadrons to test the number-of-constituent-quark (NCQ) scaling. They are also compared to recent hydrodynamic and transport model calculations. We also report on the updated measurements of D^0 nuclear modification factors $R_{\rm AA}$ and $R_{\rm CP}$ using the 2014 data. The measured D^0 $R_{\rm AA}$in central collisions is less than 1 across the entire p_T region. The D^0 yields show strong suppression at high p_T (> 6 GeV/c) in central collisions, consistent with those of light flavor hadrons.
We also report the measurements of collision centrality and p_T dependences of the $\Lambda_c^{\pm}$ production in Au+Au collisions at $\sqrt{s_{\rm NN}}$ = 200 GeV, using the HFT. The $\Lambda_c^{\pm}$ signal significance is greatly improved with the addition of the high-statistics data set collected in 2016 and the use of a supervised machine learning method for a more efficient topological reconstruction of the decay vertices. The measured $\Lambda_c^{\pm}/D^0$ ratio in 10-80% Au+Au collisions shows a significant enhancement compared to the PYTHIA prediction for $p + p$ collisions, across the measured $p_{\rm T}$ range.

1 Introduction

Relativistic heavy-ion collisions at the RHIC and LHC create a hot dense medium consisting of deconfined quarks and gluons, usually referred to as the Quark Gluon Plasma (QGP) [1, 2]. The production of heavy quarks occurs mainly during the primordial stage of heavy-ion collisions before the QGP is formed. As a consequence, the heavy quarks experience the entire evolution of the system and can be used to access information concerning the early time dynamics. Recent measurements at RHIC, based on 2014 data from the STAR experiment, have shown that D^0 mesons in minimum-bias and mid-central heavy-ion collisions exhibit significant elliptic flow [3]. The flow magnitude follows the same number-of-constituent-quark (NCQ) scaling pattern as observed for light-flavor hadrons in mid-central collisions. It is of particular interest to measure the centrality dependence of these observables and to test the NCQ scaling for charmed hadrons in different centrality classes. During 2016, STAR [4] collected an additional sample of Au+Au collisions at $\sqrt{s_{\rm NN}}$ = 200 GeV using the Heavy

*e-mail: smargeti@kent.edu

Flavor Tracker (HFT) [5, 6]. An improved precision for the elliptic flow measurements of heavy-flavor hadrons has been achieved by combining the data samples collected in 2014 and 2016, allowing more quantitative studies of the QGP properties.

The measurements of D^0 nuclear modification factor $R_{\rm AA}$ ($R_{\rm CP}$), ratio of the spectra measured in heavy-ion collisions to that in $p + p$ (peripheral heavy-ion) collisions scaled by the number of binary collisions ($N_{\rm coll}$), provide insights into the energy loss mechanism of charm quarks in the QGP medium and help constrain model parameters [7, 8]. The hadronization of charm quarks in the presence of QGP can be studied through the measurement of yield ratios of charm hadrons, particularly the $\Lambda_c^{\pm}/D^0$ (D^0 here denotes both D^0 and $\bar{D^0}$) yield ratio. Enhancement of the ratio, relative to that in $p + p$ collisions, is expected in the intermediate $p_{\rm T}$ region (2 - 6 GeV/c) if charm quarks hadronize via the coalescence mechanism in the QGP [9, 10]. The magnitude of this enhancement is sensitive to the charm quark dynamics and the presence of diquarks in the medium [9].

In these proceedings, we present an improved measurement of the $\rm D^0$ meson elliptic flow (v_2) as a function of transverse momentum (p_T) in Au+Au collisions at $\sqrt{s_{\rm NN}} = 200\,\rm GeV$. The $\rm D^0$ v_2 results are compared to those of light-flavor hadrons and to recent hydrodynamic and transport model calculations. We also present measurements of the $\Lambda_c^{\pm}/D^0$ yield ratio and the D^0 $R_{\rm AA}$ and $R_{\rm CP}$ in $\sqrt{s_{\rm NN}}$ = 200 GeV Au+Au collisions. The $\Lambda_c^{\pm}/D^0$ yield ratio is measured as a function of $p_{\rm T}$ and centrality and is compared to model calculations. The D^0 $R_{\rm AA}$ and $R_{\rm CP}$ are presented for various centrality classes as a function of $p_{\rm T}$ and compared to similar measurements for light flavor hadrons as well as model calculations.

2 Experiment and Analysis

The STAR detector at RHIC has a full azimuthal acceptance and a pseudorapidity (η) coverage of $|\eta| < 1$ [4]. The HFT [5, 6] is a high-resolution silicon detector installed close to the beam pipe and provides an excellent track pointing resolution, e.g. less than 40 μm for kaons with $p_{\rm T}$ = 1 GeV/c. This allows to place cuts on the quantities describing the decay topology of heavy flavor hadrons, which greatly enhances the signal significance. Particle identification (PID) at STAR is provided by the ionization energy loss (dE/dx) measured in the Time Projection Chamber (TPC) [11] and the velocity measured using the Time of Flight (TOF) detector [12]. About 900 M minimum-bias Au+Au events from the 2014 run and ∼1 B minimum-bias Au+Au events from the 2016 run at RHIC are used. Minimum-bias events are defined by a coincidence of signals in the east and west Vertex Position Detectors (VPD) [13] located at pseudorapidity $4.4 < |\eta| < 4.9$. The collision centrality is determined from the number of charged particles within $|\eta| < 0.5$ and corrected for triggering efficiency using a Monte Carlo Glauber simulation [14].

The D^0 and $\overline{D^0}$ mesons are reconstructed via their hadronic decay channels: D^0 ($\overline{D^0}$) $\rightarrow$ $K^-\pi^+$ ($K^+\pi^-$) (branching ratio: 3.89%, cτ ∼ 123 μm) [15] by utilizing the TOF (PID) and TPC along with the HFT for tracking. Good-quality tracks with $p_T > 0.6$ GeV/c and $|\eta| < 1$ are ensured by requiring a minimum of 20 TPC hits (out of possible 45), and with at least one hit in each layer of the Intermediate Silicon Tracker (IST) and PiXeL (PXL) components of the HFT. To enhance the signal-to-background ratio, topological variable cuts are optimized using the Toolkit for Multivariate Data Analysis (TMVA) package [16], in orthogonal cut mode.

The second-order event plane azimuthal angle (Ψ_2) is reconstructed from tracks measured in the TPC. To suppress the non-flow effects in the v_2 measurements, only tracks that are in the opposite rapidity hemisphere with at least $\Delta\eta > 0.05$ with respect to the reconstructed D^0, are used for the Ψ_2 reconstruction. The v_2 coefficients are calculated using the event-plane method [17] measuring the D^0 yields in different azimuthal intervals defined with respect to

the event plane angle ($\phi - \Psi_2$). The D^0 yields are weighted by the inverse of the reconstruction efficiency × acceptance for each interval of collision centrality. The observed v_2 is then calculated by fitting the azimuthal dependence of the D^0 yield using the function $p_0(1 + 2\, v_2^{\rm obs} \cos[2\,(\phi - \Psi_2)])$. The resolution-corrected v_2 is then obtained by dividing $v_2^{\rm obs}$ with the event-plane resolution Ψ_2 [18].

The $\Lambda_c^{\pm}$ candidates are reconstructed via the $\Lambda_c^{\pm} \to p^{\pm}K^{\mp}\pi^{\pm}$ channel using both the 2014 and 2016 datasets. The supervised learning algorithm, Boosted Decision Trees (BDT), from the TMVA is used for signal and background separation. The BDT is trained using a signal sample of $\Lambda_c^{\pm}$ decayed (using PYTHIA [19]) to $pK\pi$ triplets, with detector effects taken into account, and a background sample from wrong-sign triplets from data. The use of BDT along with the combined 2014+2016 data gives a factor of 2 improvement in the $\Lambda_c^{\pm}$ signal significance compared to the previous measurement [20].

3 Results

The averaged $v_2(p_T)$ of D^0 and $\overline{D^0}$ mesons is measured in 0-10%, 10-40% and 0-80% central Au+Au collisions at $\sqrt{s_{\rm NN}}$ = 200 GeV based on combined datasets recorded during 2014 and 2016. This provides an improvement of about a 30% in the statistical precision com-

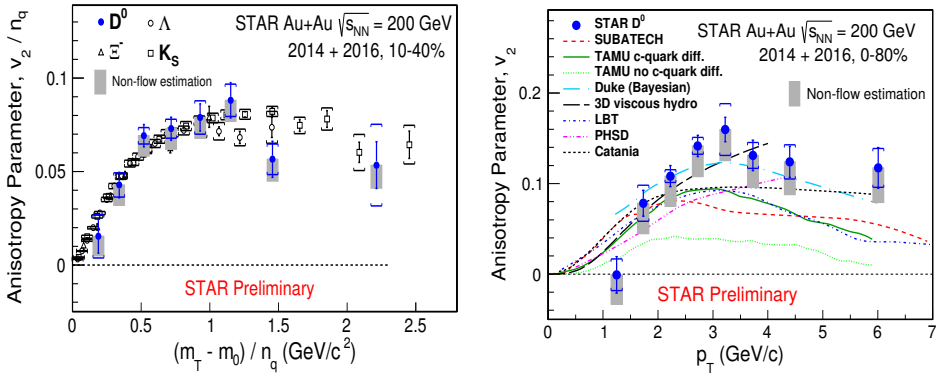

Figure 1. Left panel: v_2/n_q as a function of $(m_T - m_0)/n_q$ for D^0 and $\overline{D^0}$ mesons combined in 10-40% central Au+Au collisions at $\sqrt{s_{\rm NN}}$ = 200 GeV along with K^0_S, Λ, and Ξ [21]. Right panel: v_2 as a function of p_T for D^0 and $\overline{D^0}$ mesons combined in 0-80% Au+Au collisions compared with model calculations [22–28].

pared to previously published results using 2014 data alone [3]. The blue solid markers in the left panel of Fig. 1 present the NCQ-scaled v_2 as a function of NCQ-scaled transverse kinetic energy $(m_T - m_0)$ for D^0 mesons in 10-40% central Au+Au collisions at $\sqrt{s_{\rm NN}}$ = 200 GeV. The results are compared to light hadron species, namely the K^0_S meson and the Λ and Ξ baryons [21]. The NCQ-scaled D^0 v_2 is compatible within uncertainties with those of light hadrons for $(m_T - m_0)/n_q < 2.5$ GeV/c^2. This observation suggests that charm quarks exhibit the same strong collective behavior as light-flavor quarks, and may be close to thermal equilibrium with the medium in Au+Au collisions at $\sqrt{s_{\rm NN}}$ = 200 GeV. The right panel in Fig. 1 presents the D^0 v_2 results in 0-80% central Au+Au collisions, compared to SUBATECH [22], TAMU [23], Duke [24], 3D viscous hydro [25], LBT [26], PHSD [27], and Catania [28] model calculations. These models include different treatments of the charm

quark interactions with the medium. They also differ in initial state conditions, QGP evolution, hadronization, etc. We have performed a statistical significance test of the consistency between the data and each model, quantified by χ^2/NDF and the p value. We have found that the TAMU model without charm quark diffusion cannot describe the data, while the same model with charm quark diffusion turned-on shows better agreement. All the other models can describe the data in the measured p_T region.

The left panel of Fig. 2 shows the $\Lambda_c^{\pm}/D^0$ ratio as a function of $p_{\rm T}$ for the 10-80% centrality bin. The data shows a significant enhancement of the ratio compared to the PYTHIA prediction for $p + p$ collisions. The SHM model [29] also underpredicts the data. The Ko model (0-5%) [9] and the Greco model (0-20%) [10] calculations include coalescence of thermalized charm quarks and are closer to the measured values, but still underpredict data at higher $p_{\rm T}$. The right panel of Fig. 2 shows the $\Lambda_c^{\pm}/D^0$ ratio as a function of centrality. The $\Lambda_c^{\pm}/D^0$ ratio shows an increasing trend towards more central collisions. The measured value in the peripheral collisions is consistent with the value from $p + p$ collisions at 7 TeV measured by ALICE [30].

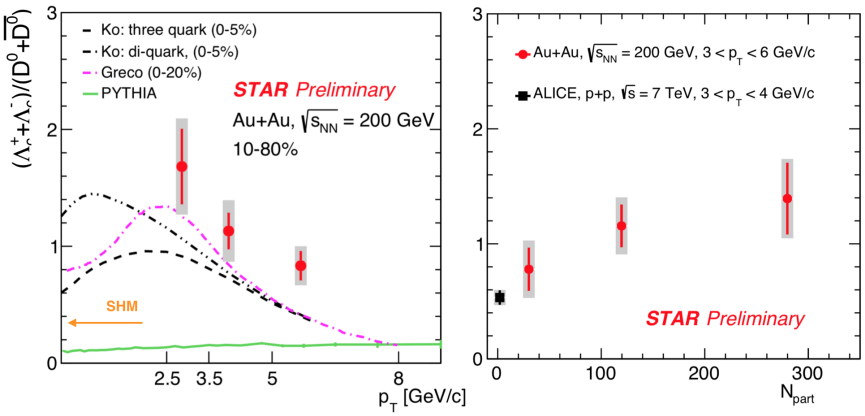

Figure 2. The $\Lambda_c^{\pm}/D^0$ ratio as a function of $p_{\rm T}$ for 10-80% centrality class (left) and as a function of $N_{\rm part}$ for $3 < p_{\rm T} < 6$ GeV/c (right), in Au+Au collisions at $\sqrt{s_{\rm NN}} = 200$ GeV. The error bars and gray bands represent statistical and systematic uncertainties, respectively.

Results of the D^0 $R_{\rm AA}$, extended down to zero $p_{\rm T}$ using the HFT data from 2014, are shown in the left panels of Fig. 3. The figures also show re-analyzed 2010/2011 results [31], which are consistent with the results from the HFT analysis of 2014 data. The D^0 $R_{\rm AA}$ values are below 1 at all $p_{\rm T}$ in central collisions. The $R_{\rm AA}$ values for $p_{\rm T} > 5$ GeV/c show significant suppression in central collisions, and the suppression decreases towards more peripheral collisions, as the system size decreases. The right panels in Fig. 3 show the D^0 $R_{\rm CP}$, relative to the 40-60% centrality bin. The $R_{\rm CP}$ values are consistent with unity for $p_{\rm T} < 2$ GeV/c, but decrease towards high $p_{\rm T}$ (> 6 GeV). The figure also shows the $R_{\rm CP}$ values for different light flavor hadrons in 200 GeV Au+Au collisions [32]. The $R_{\rm CP}$ values from light flavor hadrons are lower than those of D^0 for $p_{\rm T} < 4$ GeV/c, while they show similar levels of suppression towards higher $p_{\rm T}$. Comparisons to two model calculations which incorporate both collisional and medium induced radiative energy losses are also shown in the figure. The Duke model [33] uses a modified Langevin equation to describe the charm quark transport in the medium and radiative energy loss, while the LBT [7] uses a linearized Boltzman transport model with the higher-twist formalism for medium-induced radiative energy loss. Both models can well describe the data. The model parameters had been tuned to describe

the previous STAR measurements from [8], and the new high precision results reported here can help better constrain the model parameters.

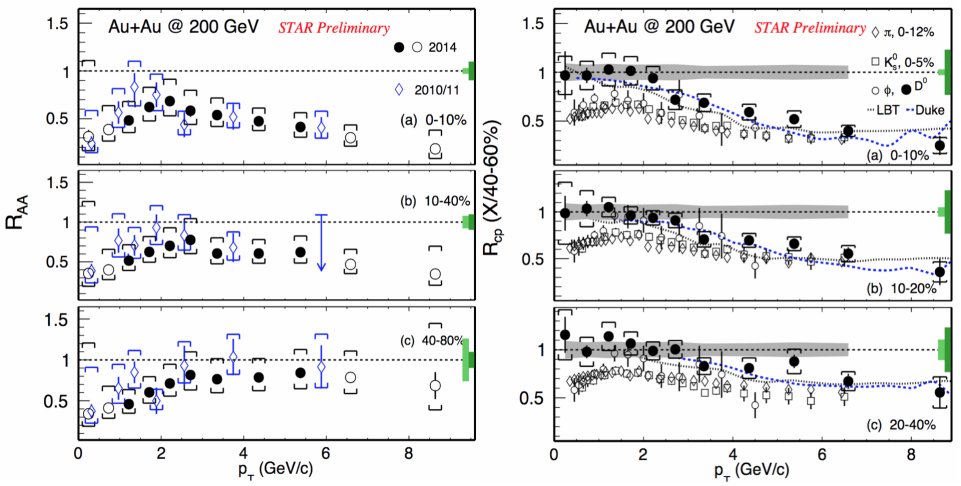

Figure 3. The D^0 R_{AA} (left) and R_{CP} values relative to 40-60% centrality bin (right) as a function of p_T for different centrality intervals. The solid circles in the left panels indicate that measured $p+p$ yields are used for calculating R_{AA} and the open circles indicate that the $p+p$ yields from an extrapolation using a Levy fit to the measured yields are used. The open diamonds are the values from re-analyzed 2010/2011 data. The error bars and brackets on the data points indicate statistical and systematic uncertainties respectively. The dark and light green boxes on the right of each panel show the global uncertainty from the reference ($p+p$ cross section uncertainty for R_{AA} and N_{coll} uncertainty for 40-60% centrality for R_{CP}) and the N_{coll} uncertainty for the given centrality bin, respectively. The shaded gray bands around 1 on the R_{CP} plots indicate the uncertainty from vertex resolution correction for the 40-60% centrality bin.

4 Conclusion

In summary, we report STAR results on the D^0 elliptic flow (v_2) as a function of p_T combining 2014 and 2016 data samples. The D^0 v_2 suggests that charm quarks may be close to thermal equilibrium in the medium. Furthermore, studies are now in progress in determining the D^0 v_2 in the peripheral collisions (40-80%), with an enlarged pseudorapidity gap to reduce non-flow effects. The measurements of the D^0 R_{AA} and R_{CP} are also presented for 200 GeV Au+Au collisions. The R_{AA} and R_{CP} values show strong suppression at high p_T in central collisions and the suppression decreases towards peripheral collisions. The R_{CP} values at high p_T (> 6 GeV/c) are consistent with those of light flavor hadrons, while they are larger for p_T < 4 GeV/c. Transport models with collisional and radiative energy losses are able to describe the measured R_{CP} values.

We also present the measurements of the $\Lambda_c^{\pm}/D^0$ ratio as functions of collision centrality and p_T in Au+Au collisions at $\sqrt{s_{NN}}$ = 200 GeV. The ratio shows a significant enhancement compared to the values from PYTHIA for $p+p$ collisions and also to SHM calculations. Model calculations with coalescence hadronization are closer to the experimental measurements, suggesting that the coalescence mechanism plays an important role in charm quark hadronization in the QGP.

References

[1] R. Rapp and H. van Hees arXiv:0803.0901.
[2] B. Muller, J. Schukraft, and B. Wyslouch, Ann. Rev. Nucl. Part. Sci. **62**, 361 (2012).
[3] L. Adamczyk *et al.* (STAR Collaboration), Phys. Rev. Lett. **118**, 212301 (2017).
[4] STAR Collaboration, Nucl. Inst. Meth. A**499**, 624 (2003).
[5] D. Beavis *et al.*, The HFT Technical Design report as prepared for the July 2011 CD2-3 review, STAR Note SN0600.
[6] G. Contin *et al.*, Nucl. Instrum. Meth. A**907**, 60 (2018)
[7] S. Cao *et al.*, Phys. Rev. C **94**, 014909 (2016).
[8] STAR Collaboraion, Phys. Rev. Lett. **113**, 142301, (2014).
[9] S. H. Lee, K. Ohnishi, S. Yasui, I.-K. Yoo and C. M. Ko Phys. Rev. Lett.**100**, 222301 (2008).
[10] S. Ghosh, S. K. Das, V. Greco, S. Sarkar and J. E. Alam, Phys. Rev. D**90** 054018 (2014).
[11] M. Anderson *et al.*, Nucl. Instr. Meth. A **499**, 659 (2003).
[12] B. Bonner *et al.*, Nucl. Instr. Meth. A **508**, 181 (2003).
[13] W. J. Llope *et al.*, Nucl. Instrum. Meth. A**522**, 252 (2004).
[14] B. Abelev *et al.*, (STAR Collaboration), Phys. Rev. C **79**, 034909 (2009).
[15] Review of Particle Physics, M. Tanabashi *et al.*, Phys. Rev. D **98**, 030001 (2018).
[16] A. Hocker *et al.*, PoS ACAT, **040** (2007).
[17] A. M. Poskanzer and S. A. Voloshin, Phys. Rev. C **58**, 1671 (1998).
[18] H. Masui *et al.*, Nucl. Instrum. Meth. A **833**, 181 (2016).
[19] T. Sjöstrand, S. Mrenna and P. Skands, Journal of High Energy Physics**2006**, 026 (2006).
[20] G. Xie (STAR Collaboration), Nucl. Phys. A **967**, 928-931, 2017.
[21] B. I. Abelev *et al.*, (STAR collaboration), Phys. Rev. C **77**, 054901 (2008).
[22] T. Song *et al.*, Phys Rev C **92**, 014910 (2015).
[23] M. He. *et al.*, Phys Rev C **86**, 014903 (2012); Phys Rev Lett **110**, 112301 (2013).
[24] S. Cao *et al.*, Phys. Rev. C **97**, 014907 (2018).
[25] L. Pang *et al.*, Phys Rev C **86**, 024911 (2012).
[26] S. Cao *et al.*, Phys Rev C **94**, 014909 (2016).
[27] T. Song *et al.*, Phys Rev C **92**, 014910 (2015).
[28] F. Scardina *et al.*, Phys Rev **96**, 044905 (2017).
[29] I. Kuznetsova and J. Rafelski, The European Physical Journal C**51** 113–133 (2007).
[30] ALICE Collaboration, arXiv:1712.09581
[31] L. Adamczyk et al. (STAR Collaboration), Phys. Rev. Lett. **113**, 142301 (2014).
[32] STAR Collaboration, Phys. Rev. Lett. **97**, 152301 (2006); Phys. Rev. C **79**, 064903 (2009); Phys. Rev. Lett. **108**, 072301
[33] Y. Xu *et al.* Phys. Rev. C. **97**, 014907 (2018).